

1 **3-5 Hz membrane potential oscillations decrease the gain of neurons in visual cortex**

2 Michael C. Einstein<sup>1,3,7</sup>, Pierre-Olivier Polack<sup>2,7</sup>, Peyman Golshani<sup>1,4,5,6</sup>

3 <sup>1</sup>Department of Neurology and Psychiatry, David Geffen School of Medicine, University of California, Los  
4 Angeles, Los Angeles, California, 90095, United States of America.

5 <sup>2</sup>Center for Molecular and Behavioral Neuroscience, Rutgers, the State University of New Jersey,  
6 Newark, New Jersey, 07102, United States of America.

7 <sup>3</sup>Neuroscience Interdepartmental Program, UCLA

8 <sup>4</sup>West Los Angeles Veterans Affairs Medical Center, Los Angeles, CA

9 <sup>5</sup>Integrative Center for Learning and Memory, UCLA

10 <sup>6</sup>Intellectual and Developmental Disability Research Center, UCLA

11 <sup>7</sup>These authors contributed equally to this work

12

13 **ABSTRACT**

14 Gain modulation is a computational mechanism critical for sensory processing. Yet, the cellular  
15 mechanisms that decrease the gain of cortical neurons are unclear. To test if low frequency  
16 subthreshold oscillations could reduce neuronal gain during wakefulness, we measured the membrane  
17 potential of primary visual cortex (V1) layer 2/3 excitatory, parvalbumin-positive (PV+), and  
18 somatostatin-positive (SOM+) neurons in awake mice during passive visual stimulation and sensory  
19 discrimination tasks. We found prominent 3-5 Hz membrane potential oscillations that reduced the gain  
20 of excitatory neurons but not the gain of PV+ and SOM+ interneurons, which oscillated synchronously  
21 with excitatory neurons and fired strongly at the peak of depolarizations. 3-5 Hz oscillation prevalence  
22 and timing were strongly modulated by visual input and the animal's behavioral response, suggesting  
23 that these oscillations are triggered to adjust sensory responses for specific behavioral contexts.  
24 Therefore, these findings reveal a novel gain reduction mechanism that adapts sensory processing to  
25 behavior.

## 26 INTRODUCTION

27 Gain modulation is a fundamental mechanism by which the brain adjusts the strength of sensory  
28 signals (Salinas & Sejnowski, 2001). During behavior, neuronal gain is tuned moment-by-moment in  
29 order to prioritize information streams important for meeting immediate behavioral demands (Harris &  
30 Thiele, 2011; Posner 1980). Notably, attention has been found to either increase (Moran & Desimone,  
31 1985; Motter, 1993; Roelfsema et al., 1998; Chalk et al., 2010) or decrease (Luck et al., 1997; Reynolds et  
32 al., 1999; Treue & Maunsell, 1996) the gain of neurons throughout the visual cortex to prioritize coding  
33 and perception of attended cues.

34 Several cellular and network mechanisms that increase the gain of sensory neurons during  
35 behavior have already been identified. Signals from the prefrontal cortex (Zhang et al., 2014; Gregoriou  
36 et al., 2014; Moore & Armstrong et al., 2003), thalamus (McAlonan et al., 2008; Purushothaman et al.,  
37 2012; Wimmer et al., 2015), and neuromodulatory centers (Polack et al., 2013; Pinto et al., 2013; Fu et  
38 al., 2014) have all been shown to increase the gain of visual cortical neurons in behaving animals.  
39 However, mechanisms that reduce the gain of sensory cortical neurons during behavior are still poorly  
40 understood. Recruitment of inhibitory GABAergic interneurons has been implicated as a mechanism that  
41 could reduce the gain of visual and auditory cortical neurons in behaving animals (Katzner et al., 2011;  
42 Disney et al., 2007; Soma et al., 2012; Olsen et al., 2012; Schneider et al., 2014). Yet, the cellular  
43 mechanisms that decrease neuronal gain in sensory cortices during behavior remain unclear.

44 We hypothesized that low frequency subthreshold oscillations could be a mechanism that  
45 reduces neuronal gain during behavior. Previously associated with sleeping and anesthetized states  
46 (Steriade et al., 1993), low frequency subthreshold oscillations have recently been observed in rodent  
47 visual (Polack et al., 2013; Bennet et al., 2013), barrel (Poulet & Petersen, 2008), auditory (Zhou et al.,  
48 2014; Schneider et al., 2014) and motor (Zagha et al., 2015) cortex neurons of awake behaving animals.  
49 During low frequency oscillations, neurons' baseline membrane potential was significantly

50 hyperpolarized (Zagha et al., 2015; Bennet et al., 2013), which could decrease the responsiveness of  
51 neurons to incoming signals (Cardin et al., 2008; Carandini & Ferster, 1997; Nowak et al., 2005).  
52 Moreover, *in vivo* (Cohen & Maunsell, 2009; Fries et al., 2001) and *in vitro* (Volgushev et al., 1998; Lampl  
53 & Yarom, 1993) experiments suggest that low frequency oscillations could provide timing templates that  
54 filter inbound sensory signals of a different time structure, which could effectively reduce the gain of  
55 sensory cortex neurons (Engel et al., 2001; Schroeder & Lakatos, 2009).

56 To investigate this hypothesis, we performed whole-cell recordings of V1 L2/3 excitatory,  
57 parvalbumin-positive (PV+), and somatostatin-positive (SOM+) neurons in awake and behaving animals.  
58 We found prominent low frequency (3-5 Hz) membrane potential oscillations in all neuron types. These  
59 3-5 Hz oscillations decreased the spontaneous firing rate and gain of excitatory neurons. Meanwhile,  
60 PV+ and SOM+ interneurons oscillated in phase with excitatory neurons, but fired strongly at the  
61 depolarized peaks of these oscillations. 3-5 Hz oscillation recruitment depended on both visual  
62 processing and behavioral state. Visual stimulation significantly increased the prevalence of oscillations,  
63 and engagement on a visual discrimination task strongly influenced the initiation, duration, and  
64 prevalence of oscillations. Altogether, our findings suggest that 3-5 Hz subthreshold oscillations are a  
65 novel mechanism for decreasing neuronal gain to tune sensory processing according to an animal's  
66 specific behavioral context.

67

## 68 **RESULTS**

### 69 **3-5 Hz Vm oscillations are highly stereotyped events that reduce the gain excitatory neurons**

70 We performed two-photon guided whole-cell Vm recordings from 40 excitatory, 6 PV+, and 7 SOM+  
71 L2/3 V1 neurons in head-fixed mice free to run or rest on a spherical treadmill (Figure 1A, B). For each  
72 recording, electrocorticogram (ECoG) activity was simultaneously acquired within the vicinity (300-500  
73  $\mu\text{m}$ ) of the patch-clamp pipette tip was simultaneously acquired. In all our recordings, we detected

74 epochs of high amplitude 3-5 Hz Vm oscillations (Figure 1A) that typically lasted for 1-2 seconds ( $1.6 \pm$   
75  $0.05$  seconds,  $n = 53$ ; Figure 1C, D). During oscillatory events, the neuron's baseline Vm substantially  
76 hyperpolarized (Mean =  $-12.0 \pm .61$  mV,  $n = 53$ ) and displayed high amplitude ( $>10$  mV) rhythmic  
77 depolarizations at  $4.14 \pm 0.06$  Hz ( $n = 53$ ; range = [2.94, 5.04]). The oscillation frequency, duration, and  
78 baseline hyperpolarization were similar in excitatory, PV+, and SOM+ neurons (one-way ANOVA  $p =$   
79  $0.55$ ; Figure 1D). However, PV+ interneurons exhibited larger amplitude depolarizing events (one-way  
80 ANOVA,  $p=0.01$ ) than excitatory (Tukey-HSD,  $p=0.04$ ) and SOM+ (Tukey-HSD,  $p = 0.01$ ) neurons did  
81 during oscillatory periods. The mean firing rates of excitatory neurons significantly decreased during the  
82 oscillation, with excitatory neurons rarely firing action potentials during the oscillatory episodes  
83 (Spontaneous firing rate- No oscillation:  $1.34 \pm .05$  Sp.s<sup>-1</sup>, Oscillation:  $0.55 \pm .02$  Sp.s<sup>-1</sup>; WSRT,  $p = 0.002$ ;  
84 Figure 1B, 2C). In contrast, PV+ and SOM+ interneurons still fired strongly at the peaks of oscillations  
85 ( $13.3 \pm 1.03$  Sp.s<sup>-1</sup>,  $n=6$ , and  $6.23 \pm 0.8$  Sp.s<sup>-1</sup>,  $n=7$ , respectively; Figure 1B, 2C).

86 3-5 Hz Vm oscillations were associated with prominent fluctuations ( $\sim 500$   $\mu$ V) in the  
87 simultaneously recorded ECoG (Figure 1A). The correlation coefficient between Vm and ECoG recordings  
88 increased during 3-5 Hz Vm oscillations from  $0.002 \pm 0.006$  to  $0.21 \pm 0.03$  ( $n=53$ , WSRT,  $p= 1.5 \times 10^{-6}$ ;  
89 Figure 1A, 1B, 2A). Given the Vm and ECoG correlation during 3-5 Hz oscillations and the similar  
90 characteristics of 3-5 Hz oscillations in excitatory, PV+, and SOM+ neurons, we hypothesized that 3-5 Hz  
91 oscillations occurred synchronously in L2/3 V1 neurons. To test this hypothesis, we measured the mean  
92 phase offset between ECoG and Vm and found no differences between excitatory, PV+, and SOM+  
93 neurons (Excitatory neurons:  $-7.5^\circ \pm 2.2^\circ$ , PV+ neurons:  $-12.3^\circ \pm 3.8$ , SOM+ neurons:  $-14.6^\circ \pm 3.1$ ; one-way  
94 ANOVA,  $p = 0.28$ ; Figure 2B). These results suggest that the Vm of excitatory, PV+ and SOM+ neurons  
95 excitatory, PV+, and SOM+ neurons oscillated in phase, depolarizing and hyperpolarizing synchronously  
96 during each oscillatory cycle.

97           Because excitatory neurons' alternate during 3-5 Hz oscillations between hyperpolarized periods  
98 and depolarized phases where they likely receive strong inhibitory inputs, we hypothesized that excitatory  
99 neurons' gain could decrease during 3-5 Hz oscillations. To investigate this hypothesis, we recorded the  
100 Vm from excitatory (n=40), PV+ (n=6), and SOM+ (n=7) neurons while mice were presented with full-  
101 screen drifting gratings (Figure 3). In the presence of oscillations, the mean firing rate of excitatory  
102 neurons was strongly reduced for the preferred visual stimulus ( $2.82 \pm 0.71 \text{ Sp.s}^{-1}$  No Osc.;  $0.75 \pm 0.18$   
103  $\text{Sp.s}^{-1}$  Osc.; n=40 neurons; WSRT,  $p = 8.1 \times 10^{-5}$ ; Figure 3C). Yet, the mean orientation selectivity index (OSI)  
104 of excitatory neurons was unchanged (WSRT,  $p = .93$ ; see methods for OSI calculation; Figure 3—figure  
105 supplement 1). Oscillations did not change PV+ (WSRT,  $p = 0.07$ ) and SOM+ (WSRT,  $p = 0.63$ ) neurons'  
106 response to the visual stimulus that evoked the greatest response (Figure 3C). In all neurons, the mean  
107 firing rate evoked by all non-preferred stimuli was not influenced by the oscillations (excitatory, WSRT,  $p$   
108  $= 0.97$ ; PV+, WSRT,  $p = 0.15$ ; SOM+, WRST,  $p = 0.16$ ). As a result, we conclude that 3-5 Hz oscillation epochs  
109 selectively reduced the gain of excitatory neurons during passive viewing.

110

111 **3-5 Hz oscillations are more prevalent during passive viewing than during spontaneous activity and**  
112 **occurred at visual stimulus offset**

113           3-5 Hz oscillations were more likely to occur while animals were shown alternations of drifting  
114 gratings and grey screens (passive viewing) than during spontaneous activity (defined as periods longer  
115 than 5 minutes where animals were shown an isoluminant grey screen; Figure 4A). The incidence rate of  
116 oscillations strongly increased in excitatory (WSRT,  $p = 1.5 \times 10^{-5}$ ), PV+ (WSRT,  $p = 0.025$ ), and SOM+  
117 (WSRT,  $p = 0.038$ ) neurons, during periods of passive visual stimulation compared to periods of  
118 spontaneous activity (Figure 4A). There was no difference in 3-5 Hz oscillation incidence between  
119 excitatory, PV+, or SOM+ during passive viewing (one-way ANOVA,  $p = 0.67$ ) and spontaneous activity  
120 (one-way ANOVA,  $p = 0.38$ ).

121 During passive viewing of either 1.5 or 3 second visual stimuli, 3-5 Hz oscillations primarily  
122 occurred after visual stimulus offset (Figure 4B and Figure 4—figure supplement 1). In all recorded  
123 neurons, the mean probability of 3-5 Hz oscillations following a 1.5 or a 3 second visual stimulus was 2.2  
124 and 2.5 fold greater, respectively, than the probability of 3-5 Hz oscillations occurring during visual stimuli  
125 (1.5 s stimuli: n=53, WSRT,  $p = 7.2 \times 10^{-9}$ ; 3 s stimuli: n = 9, WSRT,  $p = 0.004$ ; Figure 4B, Figure 4—figure  
126 supplement 1). Interestingly, the probability of an oscillation triggered during or after a passively viewed  
127 visual stimulus decreased from the first quartile of visual stimuli to the final quartile of visual stimuli (n =  
128 31 neurons; mean # stimuli presentations per recording =  $176 \pm 10$ , repeated measures one-way ANOVA,  
129  $p = 7.7e-7$ , WSRT Bonferroni Corrected,  $p = 0.0001$ ; Figure 4C). As locomotion alters L2/3 V1 neuron Vm  
130 dynamics (Polack et al., 2013; Reimer et al., 2014; Bennett et al., 2013), we also analyzed the influence of  
131 locomotion on 3-5 Hz oscillation initiation. The probability of oscillation initiation at visual stimulus offset  
132 was higher than that at visual stimulus onset, locomotion onset, and locomotion offset (WSRT Bonferroni  
133 Corrected,  $p = 0.024$ ,  $p = 0.0003$ ,  $p = 0.003$ , respectively).

134 Therefore, synchronized 3-5 Hz oscillations decreased excitatory neuron excitability and were  
135 more prevalent when visual stimuli were presented. These findings suggest a role for 3-5 Hz oscillations  
136 in modulating visual information processing. Yet, oscillations occurred primarily at the offset of visual  
137 stimulus presentations and were less frequent after repeated visual stimulation. To better understand the  
138 role of 3-5 Hz oscillations in visual processing, we decided to investigate if 3-5 Hz oscillation prevalence  
139 and timing were affected by behavior in animals engaged in a visually guided decision making task.

140

### 141 **3-5 Hz Vm oscillations occur during visual stimuli when animals performed a visually guided go/no-go** 142 **task**

143 To test if behavior modulated 3-5 Hz Vm oscillations, mice (n=17) were trained to perform a  
144 visually guided go/no-go discrimination task prior to whole-cell recordings (Figure 5A, Figure 5—figure

145 supplement 1). During the task, animals had to decide whether to lick for a water drop (go) or withhold  
146 licking (no-go) based on visual cues (go stimulus: 45° drifting gratings, no-go stimulus: 135° drifting  
147 gratings; Figure 5—figure supplement 1A). Visual stimuli were displayed for 3 seconds, and animals had  
148 to make their decision in the final second of the visual stimulus presentation (the response period).  
149 Animals reliably learned how to perform this task in 5 to 10 training sessions (Figure 5—supplement figure  
150 1B). During training, animals' licking behavior changed, especially, for go trials, where animals gradually  
151 began initiating licking prior to the response period (Figure 5—supplement figure 1C).

152           During active behavior, the onset time of 3-5 Hz oscillations was significantly different than during  
153 passive viewing and occurred almost exclusively during visual stimulus presentations (Figure 5B-D).  
154 Oscillations were initiated on average  $1.71 \pm 0.12$  seconds ( $n = 21$  neurons) after visual stimulus onset and  
155 were twice as likely to occur during visual stimulation than during inter-trial intervals ( $n=21$  neurons,  
156 WSRT,  $p = 0.026$ ; Figure 5B inset). As a result, 3-5 Hz oscillation probability during visual stimulation was  
157 significantly greater during active behavior than during passive viewing (WRST,  $p = 0.001$ ; Figure 5D left).  
158 In contrast, 3-5 Hz oscillation probability following visual stimulation was significantly greater during  
159 passive viewing than during active behavior (WRST,  $p = 0.007$ ; Figure 5D, right). The duration of oscillation  
160 epochs was slightly longer during active behavior compared to passive viewing (WRST,  $p < 0.009$ ), but  
161 oscillation frequency was unchanged (WRST,  $p = 0.8$ ; Figure 5C). Locomotion did not change oscillation  
162 prevalence or duration during active behavior ( $n=21$ , WSRT,  $p = 0.76$  and  $p = 0.56$ , respectively; Figure 5—  
163 figure supplement 2A, B). As the go and no-go visual stimuli differed by 90°, one visual stimulus (the  
164 optimal visual stimulus) typically evoked a larger response than the other (the orthogonal visual stimulus)  
165 (Figure 5E). 3-5 Hz oscillations significantly reduced visually evoked action potential firing during optimal  
166 visual stimulus presentations (WSRT,  $p = 0.001$ ), but not during the orthogonal visual stimulus  
167 presentations ( $n=21$ , WSRT,  $p = 0.68$ ; Figure 5E). In contrast to passive viewing, the prevalence of  
168 oscillations did not decrease across the behavioral sessions (repeated measures one-way ANOVA,  $p =$

169 0.099; Figure 5F). Therefore, oscillations reduced neuronal responsiveness to preferred visual stimuli  
170 during active behavior. These findings support the hypothesis that behavioral state plays a major role in  
171 modulating 3-5 Hz Vm oscillation prevalence and timing in V1.

172

### 173 **3-5 Hz Vm oscillations' prevalence and duration are modulated by behavioral response**

174 3-5 Hz Vm oscillation prevalence and timing were also investigated in the context of animals'  
175 responses during visually-guided behavior (Figure 6). 3-5 Hz oscillation prevalence was significantly higher  
176 during trials when animals correctly withheld licking (correct rejection, CR) than during trials when animals  
177 initiated a licking response either correctly (hit) or incorrectly (false-alarm, FA) (n=21, WSRT Bonferroni  
178 Corrected  $p = 0.046$ ,  $p = 0.04$ , respectively). Importantly, the visual stimulus was identical in FA and CR  
179 trials, showing that behavioral response alone and not the sensory stimulus modulated oscillation  
180 prevalence. Yet, there was no difference in oscillation prevalence between incorrect and correct  
181 behavioral response (Hit vs FA, WSRT Bonferroni Corrected,  $p = 0.9$ ; CR vs Miss, WSRT Bonferroni  
182 Corrected,  $p = .86$ ). Additionally, oscillation duration was slightly longer during CR trials than during hit  
183 trials (WSRT Bonferroni Corrected,  $p = 0.035$ ), but not FA trials (WSRT Bonferroni Corrected,  $p = 0.3$ ). The  
184 high prevalence of oscillations during CR trials disprove the hypothesis that the motor action associated  
185 with licking response triggers oscillations because licking is typically absent during CR trials. Moreover,  
186 animals did not receive rewards during CR trials, indicating that reward expectation was not the primary  
187 factor in evoking 3-5 Hz oscillations in V1.

188 3-5 Hz oscillation onset occurred after licking onset for correct (Hit, WSRT,  $p = 0.01$ ) and incorrect  
189 (FA, WSRT,  $p = 0.001$ ) go responses (Figure 6C). For trials where licking preceded the response period in  
190 correct no-go trials (CR), licking offset occurred prior to 3-5 Hz oscillation onset (WSRT,  $p = 0.031$ ). There  
191 was no difference in oscillation onset time across behavioral responses (Repeated Measures one-way



192 ANOVA,  $p = 0.35$ ). Therefore, 3-5 Hz oscillations followed the animal's response to the go/no-go visual  
193 cue.

194

195 **3-5 Hz oscillations are absent from V1 L2/3 neurons when animals perform an analogous auditory**  
196 **decision making task**

197 To test whether 3-5 Hz oscillations in V1 were specific to processing of visual information during  
198 visual discrimination, V1 neurons' Vm was recorded as animals performed an analogous auditory go/no-  
199 go task (Figure 7). All task parameters were identical with the exception that animals based their decision  
200 on auditory cues (5 kHz – go, 10 kHz – no-go; Figure 7A) and no visual stimuli were shown. During the  
201 auditory task, a monitor was placed in the identical position as during the visual task, and an isoluminant  
202 grey screen was displayed throughout the recording to provide equal illumination as during the visual  
203 task. Oscillations occurred much less frequently when animals based their decision on auditory cues  
204 instead of visual cues (Figure 7B, C, & D). The probability of a 3-5 Hz oscillation occurring during stimulus  
205 presentations increased approximately four-fold during the visual task than the auditory task (auditory  $n$   
206 = 7, visual  $n = 21$ ,  $p = 0.003$  WRST). Yet, no difference was detected in oscillation duration (WRST,  $p = 0.27$ )  
207 and oscillation onset latency from stimulus onset (WRST,  $p = 0.64$ ) between animals performing the visual  
208 and auditory tasks (Figure 7D). Finally, animals discriminated between auditory and visual stimuli equally  
209 well (WRST,  $p = 0.37$ ), indicating that animal performance was not different during visual and auditory  
210 tasks. Taken together, these results suggest that 3-5 Hz oscillations in V1 neurons were primarily  
211 associated with visual information processing as opposed non-specific decision making and motor outputs  
212 associated with the task.

213

214 **DISCUSSION**

215 We performed two-photon guided whole-cell recordings in awake mice to investigate a novel gain  
216 reduction mechanism in L2/3 V1 neurons of mice. We found that 3-5 Hz subthreshold oscillations  
217 decreased the gain of excitatory neurons but not PV+ and SOM+ interneurons, which oscillated in phase  
218 with excitatory neurons and fired strongly at the depolarized peaks of oscillations. In addition, oscillation  
219 recruitment relied both on visual processing and the animal's behavioral state. As a result, 3-5 Hz  
220 subthreshold oscillations represent a gain reduction mechanism which adjusts neuronal activity according  
221 to an animal's sensory and behavioral context.

222 3-5 Hz subthreshold oscillations may decrease the gain of excitatory neurons to sensory cues in  
223 at least one of the following ways: (a) the hyperpolarized Vm baseline during oscillatory sequences likely  
224 contributes to decrease the gain of the neurons by reducing the response magnitude to incoming signals  
225 (Cardin et al., 2008; Carandini & Ferster, 1997; Nowak et al., 2005); (b) during the depolarizing phases of  
226 the oscillations where excitatory neurons' Vm is closest to reaching spike threshold, excitatory neurons  
227 received strong perisomatic and dendritic inhibition from GABAergic PV+ and SOM+ neurons, respectively  
228 (Taniguchi, 2014; Figure 2); (c) sensory signals out of phase with 3-5 Hz oscillations could filter inbound  
229 sensory signals of a different time structure (Engel et al., 2001; Schroeder & Lakatos, 2009; Lakatos et al.,  
230 2008). Considering the combination of these three mechanisms, 3-5 Hz subthreshold oscillations  
231 represent a potent combination of inhibitory strategies to reduce the gain of excitatory sensory neurons.

232 3-5 Hz subthreshold oscillations may be important in other cortical circuits as they have been  
233 observed in barrel (Poulet & Petersen, 2008), auditory (Zhou et al., 2014; Schneider et al., 2014) and motor  
234 (Zagha et al., 2015) cortex neurons in awake behaving mice. In particular, Zagha and colleagues  
235 investigated the distribution of the Vm of M1 neurons during 3-5 Hz subthreshold oscillations and  
236 observed an approximate 8 mV hyperpolarization of the mean membrane potential, which reduced the  
237 probability that the M1 neuron's Vm would cross the spike threshold. Simultaneous with the subthreshold  
238 oscillations, 3-8 Hz LFP power was significantly higher in S1 and M1 during miss trials while animals

239 performed a whisker deflection detection task. Zagha and colleagues hypothesized that these oscillations  
240 disorganized task-relevant circuitry by correlating activity in opposing neural ensembles. As a result, 3-5  
241 Hz subthreshold oscillations likely exist beyond the visual cortex and could perform a similar function in  
242 other sensory cortices.

243 The behavioral significance of 3-5 Hz subthreshold oscillations in visual cortex may be to reduce  
244 processing of behaviorally irrelevant visual stimuli. Accordingly, we found that oscillations were most  
245 prevalent after animals had made their decision during visual discrimination (Figure 6), a point in the task  
246 when additional visual inputs were irrelevant to completing the task. This finding alone would predict that  
247 oscillations would occur whenever animals do not require visual input during decision making, such as  
248 when animals perform an auditory discrimination task. Instead, we found that 3-5 Hz oscillations were  
249 not evoked when animals did not engage in visual cues (Figure 7), illustrating that engagement with visual  
250 stimuli is critical for eliciting oscillations. In fact, the level of animal engagement with visual stimuli may  
251 influence the prevalence of oscillations given that oscillation prevalence decreased over time during  
252 passive viewing (Figure 4C) but not during active visual discrimination (Figure 5G). Therefore, we propose  
253 that 3-5 Hz subthreshold oscillations may be evoked during visual information processing to decrease the  
254 gain of V1 neurons at times when visual cues are no longer behaviorally relevant.

255 Such a mechanism could be particularly useful during other behaviors such as attention and  
256 working memory. When non-human primates ignore visual cues during attention tasks, neurons in V4  
257 increase their correlated firing at frequencies between 3 and 5 Hz, spiking synchronizes within low  
258 frequency bands (<10 Hz) of the LFP (Mitchell et al., 2009; Fries et al., 2001), and LFP power between 3-5  
259 Hz increases (Fries et al., 2008). During visually-guided working memory tasks in non-human primates,  
260 prominent high-amplitude 4-8 Hz LFP oscillations appear in visual cortex and synchronize single-unit firing  
261 to the peaks of the oscillations during the delay period (Lee et al., 2005; Liebe et al., 2012). If coordinated  
262 subthreshold oscillations are responsible for producing these LFP and spiking patterns, their role may be

263 to exclude processing of unattended cues during attention and task irrelevant visual information during  
264 working memory.

265 3-5 Hz oscillation generation could be the result of resonant activity in the thalamocortical  
266 network. The thalamocortical loop is responsible for generating several natural and pathological  
267 oscillations, including oscillations in the 3-5 Hz range (Steriade et al., 1993, Destexhe & Sejnowski, 2003,  
268 Buzsáki & Draughn, 2004). Thalamocortical neurons switch between tonic spiking and oscillatory burst  
269 firing depending on their resting membrane potential, a phenomenon largely due to low-voltage activated  
270 T-type  $Ca^{2+}$  channels (Jahnsen & Llinás, 1984; Contreras, 2006; Halassa, 2012). Neuromodulatory inputs,  
271 including cholinergic and monoaminergic sources, regulate the resting membrane potential of thalamic  
272 neurons to allow or block the generation of oscillations (McCormick, 1989; Saper et al., 2005; Steriade et  
273 al., 1993). Given that neuromodulatory tone can play a key role in modulating visual processing (Polack et  
274 al., 2013; Pinto et al., 2013; McCormick et al., 1993; Disney et al., 2007; Chubykin et al., 2013), it is  
275 conceivable that 3-5 Hz oscillations could be caused by a change in thalamic neuromodulation, allowing  
276 thalamocortical neurons to hyperpolarize and enter a burst state capable of generating 3-5 Hz oscillations.

277 In conclusion, it is possible that the mechanism identified in this study may modulate cortical  
278 computations in a variety of cortical circuits during several different behaviors. More work will be needed  
279 to fully understand the cellular and network properties and functional significance of subthreshold 3-5 Hz  
280 oscillations. In particular, further studies will focus on understanding how and where these oscillations  
281 are generated. Finally, it will be important to record subthreshold oscillations in other brain areas during  
282 different behavioral tasks to confirm whether this mechanism is indeed ubiquitous in cortical circuits.

283

## 284 **MATERIALS AND METHODS**

### 285 **Surgery**

286 All experimental procedures were approved by the University of California, Los Angeles Office  
287 for Animal Research Oversight and by the Chancellor's Animal Research Committees. Adult (2–12  
288 months old) male and female C57Bl6/J, SOM-Cre (JAX number 013044) × Ai9 (JAX number 007909), and  
289 PV-Cre (JAX number 008069) × Ai9 mice were anesthetized with isoflurane (3–5% induction, 1.5%  
290 maintenance) ten minutes after injection of a systemic analgesic (carprofen, 5 mg per kg of body weight)  
291 and placed in a stereotaxic frame. Mice were kept at 37°C at all times using a feedback-controlled  
292 heating pad. Pressure points and incision sites were injected with lidocaine (2%), and eyes were  
293 protected from desiccation using artificial tear ointment. The skin above the skull was incised, a custom-  
294 made lightweight metal head holder was implanted on the skull using Vetbond (3M) and a recording  
295 chamber was built using dental cement (Ortho-Jet, Lang). Mice had a recovery period from surgery of  
296 five days, during which they were administered amoxicillin (0.25 mg per ml in drinking water through  
297 the water supply). After the recovery period, mice were habituated to head fixation on the spherical  
298 treadmill. On the day of the recording, mice were anesthetized with isoflurane. To fix the ground wire, a  
299 small craniotomy (.5 mm diameter) was made above the right cerebellum and a silver wire was  
300 implanted at the surface of the craniotomy and fixed with dental cement. A circular craniotomy  
301 (diameter = 3 mm) was performed above V1 and a 3-mm diameter coverslip drilled with a 500-µm  
302 diameter hole was placed over the dura, such that the coverslip fit entirely in the craniotomy and was  
303 flush with the skull surface. The coverslip was kept in place using Vetbond and dental cement, and the  
304 recording chamber was filled with cortex buffer containing 135 mM NaCl, 5 mM KCl, 5 mM HEPES, 1.8  
305 mM CaCl<sub>2</sub> and 1 mM MgCl<sub>2</sub>. The head-bar was fixed to a post and the mouse was placed on the  
306 spherical treadmill to recover from anesthesia. All recordings were performed at least two hours after  
307 the end of anesthesia, when the mouse was alert and could actively participate in the behavioral task.

308

309 **Electrophysiological recordings**

310 Long-tapered micropipettes made of borosilicate glass (1.5-mm outer diameter, 0.86-mm inner  
311 diameter, Sutter Instrument) were pulled on Sutter Instruments P-1000 pipette puller to a resistance of  
312 3–7 M $\Omega$ , and filled with an internal solution containing 115 mM potassium gluconate, 20 mM KCl, 10  
313 mM HEPES, 10 mM phosphocreatine, 14 mM ATP-Mg, 0.3 mM GTP, and 0.01–0.05 mM Alexa-594 (for  
314 experiments with C57Bl/6 mice) or Alexa-488 (for interneuron recordings). Pipettes were lowered into  
315 the brain under two-photon imaging guidance performed with a Sutter MOM microscope using a Ti-  
316 Sapphire Ultra-2 laser (Coherent) at 800 nm and a 40 $\times$  0.8 NA Olympus water-immersion objective.  
317 Images were acquired using Scanimage 3.2 software (Pologruto et al., 2003) Whole-cell current-clamp  
318 recordings were performed using the bridge mode of an Axoclamp 2A amplifier (Molecular Devices),  
319 then further amplified and low-pass filtered at 5 kHz using a Warner Instruments amplifier (LPF 202A).  
320 Recordings typically lasted 30 min (range 5 to 50 min). Recordings or parts of recordings with unstable  
321 membrane potential and/or action potentials < 35 mV were excluded from analysis. ECoG recordings  
322 were performed with an alternating/direct current differential amplifier (Model 3000, A-M system) and  
323 band-pass filtered at 0.1–3,000 Hz. Analog signals were digitized at 12 kHz with WinEDR (Strathclyde  
324 University) using a NIDAQ card (National Instruments). We recorded 40 excitatory, 6 PV+, and 7 SOM+  
325 neurons from 29, 5, and 6 untrained mice, respectively, in separate experiments to ascertain 3-5 Hz  
326 oscillation activity during spontaneous behavior and passive viewing. We recorded 21 neurons from 17  
327 trained mice in separate experiments to ascertain 3-5 Hz oscillation activity during visual and auditory  
328 discrimination.

329

### 330 **Visual Stimulus Presentation**

331 A 40-cm diagonal LCD monitor was placed in the monocular visual field of the mouse at a  
332 distance of 30 cm, contralateral to the craniotomy. Custom-made software developed with  
333 Psychtoolbox in MATLAB was used to display drifting sine wave gratings (series of 12 orientations spaced

334 by 30 degrees randomly permuted, temporal frequency = 2 Hz, spatial frequency = 0.04 cycle per  
335 degree, contrast = 100%). For passive viewing, the presentation of each orientation lasted 1.5 or 3 s and  
336 was followed by the presentation of a gray isoluminant screen for an additional 1.5 or 3 s, respectively.  
337 The electrophysiological signal was digitized simultaneously with two analog signals coding for the  
338 spatial and temporal properties of the grating. The treadmill motion was measured every 25 ms (40 Hz)  
339 by an optical mouse whose signal was converted into two servo pulse analog signals (front-back and left-  
340 right) using an external PIC microcontroller, and acquired simultaneously with the electrophysiological  
341 data.

342

### 343 **Training**

344 C57Bl/6J mice (Jackson Labs) with head-bar implants were water-deprived to 90% of their body  
345 weight and acclimated to head-fixation on a spherical treadmill in custom-built, sound-proof training  
346 rigs. Each rig was equipped with a monitor (Dell), water dispenser with a built-in lickometer (to monitor  
347 licking, infrared beam break) (Island-Motion), an infrared camera (Microsoft), and stereo speakers  
348 (Logitech). In addition, data acquisition boards (National Instruments) were used to actuate water  
349 delivery and vacuum reward retrieval as well as monitor animal licking. Data acquisition boards and the  
350 monitor were connected to a laptop (Dell), which ran the custom made training program (MATLAB).  
351 Once animals reached the target weight, they were trained to discriminate visual stimuli or auditory. In  
352 the visual discrimination task, drifting sine-wave gratings at one orientation were paired with a water  
353 reward, and the animal was expected to lick (go). Orthogonal drifting gratings signaled the absence of  
354 reward, and the animal was expected to withhold licking (no-go) during these trials. In the auditory  
355 discrimination task, a 100 dB 5 kHz pure tone indicated Go trials and a 100 dB 10 kHz pure tone  
356 indicated No-Go trials.

357           Each trial lasted three seconds. The visual or auditory stimulus was present for the duration of  
358 the trial. When the stimulus instructed the animal to lick, water was dispensed two seconds after  
359 stimulus onset. No water was dispensed in the no-lick condition. Licking was only assessed during the  
360 final second of the trial. If the animal responded correctly, the inter-trial interval (ITI) was 3 seconds. If  
361 the animal responded incorrectly, the ITI was increased to 9.5 seconds as negative reinforcement. If the  
362 animal missed a reward, the reward was removed by vacuum at the end of the trial. Animals performed  
363 300-500 trials daily.

364           Performance was measured using the  $D'$  statistic ( $D' = \text{norminv}(\text{fraction trials with correct licking})$   
365  $- \text{norminv}(\text{fraction trials with incorrect licking})$ ,  $\text{norminv}$  = inverse of the normal cumulative distribution  
366 function), which compares the standard deviation from chance performance during lick and no-lick trials  
367 (chance  $D' = 0$ ). Animals were considered experts if their sessions average  $D' > 1.7$  (probability of chance  
368 behavior  $< 0.1\%$ , Monte Carlo Simulation).

369

## 370 **Analysis**

371           Data analysis was performed using custom made routines in MATLAB. The 3-5 Hz oscillations  
372 were defined as regular low frequency and high-amplitude oscillations of the Vm superimposed on a  
373 steady hyperpolarizing envelope (see examples in Figs. 1b, 3a, 3b, 5a, and 7a). The Vm baseline was  
374 defined as the mean of the bottom 20<sup>th</sup> percentile of the Vm distribution, and the change in Vm baseline  
375 during oscillations was defined as the baseline during the oscillation epoch minus the baseline one  
376 second prior to the oscillation epoch. The spontaneous firing rate during the oscillation was calculated  
377 as the total number of action potential recorded during the oscillation divided by the duration of the  
378 oscillation. This was then compared to the firing rate measured during the 1.5 seconds preceding the  
379 oscillation. Phase offset was obtained by calculating the difference in time between positive peaks in  
380 low pass filtered ( $-3 \text{ dB @ } 10 \text{ Hz}$ ) ECoG and Vm signals measured in degrees during oscillatory epochs.



381 The orientation selectivity index (OSI) in excitatory neurons was calculated using the following equation  
382 (Mazurek et al., 2014):  $osi = ||V|| = \left| \frac{\sum F(\theta)e^{i\theta}}{\sum F(\theta)} \right|$ . To compare firing rates evoked by visual stimuli  
383 during passive viewing and behavior, trials with the presence of an oscillatory epoch at any point of the  
384 trial were compared to trials without any oscillations. Oscillation incidence was defined as the number  
385 of oscillations occurring over all spontaneous activity or passive viewing divided by the total time.  
386 Probability of oscillation and oscillation onset was defined as the probability of the event occurring in a  
387 given time bin. During the behavioral task, the optimal visual stimulus was defined as the stimulus that  
388 had a greater mean evoked firing rate.

389

### 390 **Statistics**

391 Unless stated otherwise, statistical significance was calculated by Wilcoxon Signed Rank Test  
392 (WSRT), Wilcoxon Rank-Sum Test (WRST), One Way Analysis of Variance (ANOVA), and Repeated  
393 Measures one-way ANOVA. Scale bars and shading around means represent SEM unless indicated.  
394 Wilcoxon tests were performed in MATLAB and ANOVA tests were performed in SPSS Statistics version  
395 21 (IBM).

396

### 397 **ACKNOWLEDGEMENTS**

398 The authors declare no competing financial interest. We thank all the members of the Golshani Lab for  
399 their support and insightful comments in reviewing the data and manuscript. This work was supported  
400 by NIH grants 1R01-MH101198-01 and R01-MH105427-A1. M.E. is supported by a National Research  
401 Service Award F31EY025185-02. P-O. P. performed the electrophysiological recordings in non-behaving  
402 mice. M.E. and P-O.P. performed the electrophysiological recordings in behaving mice. M.E., P-O.P., and  
403 P.G. designed the study. M.E. and P-O.P. designed the behavioral paradigm. M.E. analyzed the data.

404 M.E. wrote the manuscript with contribution from P.G. and P-O.P. Correspondence and requests for  
405 materials should be addressed to [pgolshani@mednet.ucla.edu](mailto:pgolshani@mednet.ucla.edu).

406

## 407 REFERENCES

- 408 Bennett, C., Arroyo, S., & Hestrin, S. (2013). Subthreshold Mechanisms Underlying State-Dependent  
409 Modulation of Visual Responses. *Neuron*, *80*(2), 350–357. doi:10.1016/j.neuron.2013.08.007
- 410 Carandini, M., & Ferster, D. (1997). A Tonic Hyperpolarization Underlying Contrast Adaptation in Cat  
411 Visual Cortex. *Science*, *276*(5314), 949–952. doi:10.1126/science.276.5314.949
- 412 Cardin, J. A., Palmer, L. A., & Contreras, D. (2008). Cellular mechanisms underlying stimulus-dependent  
413 gain modulation in primary visual cortex neurons in vivo. *Neuron*, *59*(1), 150–160.  
414 doi:10.1016/j.neuron.2008.05.002
- 415 Chalk, M., Herrero, J. L., Gieselmann, M. A., Delicato, L. S., Gotthardt, S., & Thiele, A. (2010). Attention  
416 reduces stimulus-driven gamma frequency oscillations and spike field coherence in V1. *Neuron*,  
417 *66*(1), 114–125. doi:10.1016/j.neuron.2010.03.013
- 418 Chubykin, A. A., Roach, E. B., Bear, M. F., & Shuler, M. G. H. (2013). A cholinergic mechanism for reward  
419 timing within primary visual cortex. *Neuron*, *77*(4), 723–735. doi:10.1016/j.neuron.2012.12.039
- 420 Cohen, M. R., & Maunsell, J. H. R. (2009). Attention improves performance primarily by reducing  
421 interneuronal correlations. *Nature Neuroscience*, *12*(12), 1594–1600. doi:10.1038/nn.2439
- 422 Contreras, D. (2006). The role of T-channels in the generation of thalamocortical rhythms. *CNS &*  
423 *Neurological Disorders Drug Targets*, *5*(6), 571–585.
- 424 Destexhe, A., & Sejnowski, T. J. (2003). Interactions Between Membrane Conductances Underlying  
425 Thalamocortical Slow-Wave Oscillations. *Physiological Reviews*, *83*(4), 1401–1453.  
426 doi:10.1152/physrev.00012.2003
- 427 Disney, A. A., Aoki, C., & Hawken, M. J. (2007). Gain Modulation by Nicotine in Macaque V1. *Neuron*,  
428 *56*(4), 701–713. doi:10.1016/j.neuron.2007.09.034
- 429 Engel, A. K., Fries, P., & Singer, W. (2001). Dynamic predictions: Oscillations and synchrony in top-down  
430 processing. *Nature Reviews Neuroscience*, *2*(10), 704–716. doi:10.1038/35094565
- 431 Fries, P., Neuenschwander, S., Engel, A. K., Goebel, R., & Singer, W. (2001). Rapid feature selective  
432 neuronal synchronization through correlated latency shifting. *Nature Neuroscience*, *4*(2), 194–200.  
433 doi:10.1038/84032
- 434 Fries, P., Womelsdorf, T., Oostenveld, R., & Desimone, R. (2008). The Effects of Visual Stimulation and  
435 Selective Visual Attention on Rhythmic Neuronal Synchronization in Macaque Area V4. *The Journal*  
436 *of Neuroscience*, *28*(18), 4823–4835. doi:10.1523/JNEUROSCI.4499-07.2008
- 437 Fu, Y., Tucciarone, J. M., Espinosa, J. S., Sheng, N., Darcy, D. P., Nicoll, R. A., ... Stryker, M. P. (2014). A  
438 cortical circuit for gain control by behavioral state. *Cell*, *156*(6), 1139–1152.  
439 doi:10.1016/j.cell.2014.01.050
- 440 Gregoriou, G. G., Rossi, A. F., Ungerleider, L. G., & Desimone, R. (2014). Lesions of prefrontal cortex  
441 reduce attentional modulation of neuronal responses and synchrony in V4. *Nature Neuroscience*,  
442 *17*(7), 1003–1011. doi:10.1038/nn.3742
- 443 Halassa, M. M. (2011). Thalamocortical dynamics of sleep: roles of purinergic neuromodulation.  
444 *Seminars in Cell & Developmental Biology*, *22*(2), 245–251. doi:10.1016/j.semcdb.2011.02.008
- 445 Harris, K. D., & Thiele, A. (2011). Cortical state and attention. *Nature Reviews Neuroscience*, *12*(9), 509–  
446 523. doi:10.1038/nrn3084

- 447 Jahnsen, H., & Llinás, R. (1984). Electrophysiological properties of guinea-pig thalamic neurones: an in  
448 vitro study. *The Journal of Physiology*, *349*, 205–226.
- 449 Katzner, S., Busse, L., & Carandini, M. (2011). GABAA inhibition controls response gain in visual cortex.  
450 *The Journal of Neuroscience*, *31*(16), 5931–5941. doi:10.1523/JNEUROSCI.5753-10.2011
- 451 Lakatos, P., Karmos, G., Mehta, A. D., Ulbert, I., & Schroeder, C. E. (2008). Entrainment of neuronal  
452 oscillations as a mechanism of attentional selection. *Science (New York, N. Y.)*, *320*(5872), 110–113.  
453 doi:10.1126/science.1154735
- 454 Lampl, I., & Yarom, Y. (1993). Subthreshold oscillations of the membrane potential: a functional  
455 synchronizing and timing device. *Journal of Neurophysiology*, *70*(5), 2181–2186.
- 456 Lee, H., Simpson, G. V., Logothetis, N. K., & Rainer, G. (2005). Phase Locking of Single Neuron Activity to  
457 Theta Oscillations during Working Memory in Monkey Extrastriate Visual Cortex. *Neuron*, *45*(1),  
458 147–156. doi:10.1016/j.neuron.2004.12.025
- 459 Liebe, S., Hoerzer, G. M., Logothetis, N. K., & Rainer, G. (2012). Theta coupling between V4 and  
460 prefrontal cortex predicts visual short-term memory performance. *Nature Neuroscience*, *15*(3), 456–  
461 462. doi:10.1038/nn.3038
- 462 Luck, S. J., Chelazzi, L., Hillyard, S. A., & Desimone, R. (1997). Neural Mechanisms of Spatial Selective  
463 Attention in Areas V1, V2, and V4 of Macaque Visual Cortex. *Journal of Neurophysiology*, *77*(1), 24–  
464 42.
- 465 Mazurek, M., Kager, M., & Van Hooser, S. D. (2014). Robust quantification of orientation selectivity and  
466 direction selectivity. *Frontiers in Neural Circuits*, *8*. doi:10.3389/fncir.2014.00092
- 467 McAlonan, K., Cavanaugh, J., & Wurtz, R. H. (2008). Guarding the gateway to cortex with attention in  
468 visual thalamus. *Nature*, *456*(7220), 391–394. doi:10.1038/nature07382
- 469 McCormick, D. A. (1989). Cholinergic and noradrenergic modulation of thalamocortical processing.  
470 *Trends in Neurosciences*, *12*(6), 215–221.
- 471 McCormick, D. A., Wang, Z., & Huguenard, J. (1993). Neurotransmitter control of neocortical neuronal  
472 activity and excitability. *Cerebral Cortex (New York, N. Y.: 1991)*, *3*(5), 387–398.
- 473 Mitchell, J. F., Sundberg, K. A., & Reynolds, J. H. (2009). Spatial attention decorrelates intrinsic activity  
474 fluctuations in macaque area V4. *Neuron*, *63*(6), 879–888. doi:10.1016/j.neuron.2009.09.013
- 475 Moore, T., & Armstrong, K. M. (2003). Selective gating of visual signals by microstimulation of frontal  
476 cortex. *Nature*, *421*(6921), 370–373. doi:10.1038/nature01341
- 477 Moran, J., & Desimone, R. (1985). Selective attention gates visual processing in the extrastriate cortex.  
478 *Science (New York, N. Y.)*, *229*(4715), 782–784.
- 479 Motter, B. C. (1993). Focal attention produces spatially selective processing in visual cortical areas V1,  
480 V2, and V4 in the presence of competing stimuli. *Journal of Neurophysiology*, *70*(3), 909–919.
- 481 Nowak, L. G., Sanchez-Vives, M. V., & McCormick, D. A. (2005). Role of Synaptic and Intrinsic Membrane  
482 Properties in Short-Term Receptive Field Dynamics in Cat Area 17. *The Journal of Neuroscience*,  
483 *25*(7), 1866–1880. doi:10.1523/JNEUROSCI.3897-04.2005
- 484 Olsen, S. R., Bortone, D. S., Adesnik, H., & Scanziani, M. (2012). Gain control by layer six in cortical  
485 circuits of vision. *Nature*, *483*(7387), 47–52. doi:10.1038/nature10835
- 486 Pinto, L., Goard, M. J., Estandian, D., Xu, M., Kwan, A. C., Lee, S.-H., ... Dan, Y. (2013). Fast modulation of  
487 visual perception by basal forebrain cholinergic neurons. *Nature Neuroscience*, *16*(12), 1857–1863.  
488 doi:10.1038/nn.3552
- 489 Posner, M. I. (1980). Orienting of attention. *The Quarterly Journal of Experimental Psychology*, *32*(1), 3–  
490 25.
- 491 Poulet, J. F. A., & Petersen, C. C. H. (2008). Internal brain state regulates membrane potential synchrony  
492 in barrel cortex of behaving mice. *Nature*, *454*(7206), 881–885. doi:10.1038/nature07150
- 493 Purushothaman, G., Marion, R., Li, K., & Casagrande, V. A. (2012). Gating and control of primary visual  
494 cortex by pulvinar. *Nature Neuroscience*, *15*(6), 905–912. doi:10.1038/nn.3106

- 495 Reimer, J., Froudarakis, E., Cadwell, C. R., Yatsenko, D., Denfield, G. H., & Tolias, A. S. (2014). Pupil  
496 Fluctuations Track Fast Switching of Cortical States during Quiet Wakefulness. *Neuron*, *84*(2), 355–  
497 362. doi:10.1016/j.neuron.2014.09.033
- 498 Reynolds, J. H., Chelazzi, L., & Desimone, R. (1999). Competitive mechanisms subserve attention in  
499 macaque areas V2 and V4. *The Journal of Neuroscience*, *19*(5), 1736–1753.
- 500 Roelfsema, P. R., Lamme, V. A., & Spekreijse, H. (1998). Object-based attention in the primary visual  
501 cortex of the macaque monkey. *Nature*, *395*(6700), 376–381. doi:10.1038/26475
- 502 Salinas, E., & Sejnowski, T. J. (2001). Gain Modulation in the Central Nervous System: Where Behavior,  
503 Neurophysiology, and Computation Meet. *The Neuroscientist*, *7*(5), 430–440.
- 504 Saper, C. B., Scammell, T. E., & Lu, J. (2005). Hypothalamic regulation of sleep and circadian rhythms.  
505 *Nature*, *437*(7063), 1257–1263. doi:10.1038/nature04284
- 506 Schneider, D. M., Nelson, A., & Mooney, R. (2014). A synaptic and circuit basis for corollary discharge in  
507 the auditory cortex. *Nature*, *513*(7517), 189–194. doi:10.1038/nature13724
- 508 Schroeder, C. E., & Lakatos, P. (2009). Low-frequency neuronal oscillations as instruments of sensory  
509 selection. *Trends in Neurosciences*, *32*(1), 9–18. doi:10.1016/j.tins.2008.09.012
- 510 Soma, S., Shimegi, S., Suematsu, N., & Sato, H. (2013). Cholinergic modulation of response gain in the rat  
511 primary visual cortex. *Scientific Reports*, *3*. doi:10.1038/srep01138
- 512 Steriade, M., McCormick, D. A., & Sejnowski, T. J. (1993). Thalamocortical oscillations in the sleeping and  
513 aroused brain. *Science*, *262*(5134), 679–685. doi:10.1126/science.8235588
- 514 Taniguchi, H. (2014). Genetic dissection of GABAergic neural circuits in mouse neocortex. *Frontiers in*  
515 *Cellular Neuroscience*, *8*, 8. doi:10.3389/fncel.2014.00008
- 516 Treue, S., & Maunsell, J. H. (1996). Attentional modulation of visual motion processing in cortical areas  
517 MT and MST. *Nature*, *382*(6591), 539–541. doi:10.1038/382539a0
- 518 Volgushev, M., Chistiakova, M., & Singer, W. (1998). Modification of discharge patterns of neocortical  
519 neurons by induced oscillations of the membrane potential. *Neuroscience*, *83*(1), 15–25.
- 520 Wimmer, R. D., Schmitt, L. I., Davidson, T. J., Nakajima, M., Deisseroth, K., & Halassa, M. M. (2015).  
521 Thalamic control of sensory selection in divided attention. *Nature*, *526*(7575), 705–709.  
522 doi:10.1038/nature15398
- 523 Zaghera, E., Ge, X., & McCormick, D. A. (2015). Competing Neural Ensembles in Motor Cortex Gate Goal-  
524 Directed Motor Output. *Neuron*, *88*(3), 565–577. doi:10.1016/j.neuron.2015.09.044
- 525 Zhang, S., Xu, M., Kamigaki, T., Hoang Do, J. P., Chang, W.-C., Jenvay, S., ... Dan, Y. (2014). Selective  
526 attention. Long-range and local circuits for top-down modulation of visual cortex processing. *Science*  
527 (*New York, N.Y.*), *345*(6197), 660–665. doi:10.1126/science.1254126
- 528 Zhou, M., Liang, F., Xiong, X. R., Li, L., Li, H., Xiao, Z., ... Zhang, L. I. (2014). Scaling down of balanced  
529 excitation and inhibition by active behavioral states in auditory cortex. *Nature Neuroscience*, *17*(6),  
530 841–850. doi:10.1038/nn.3701

531  
532 **FIGURE LEGENDS**

533 **Figure 1. V1 L2/3 excitatory, PV+, and SOM+ neurons' Vm spontaneously undergo high amplitude 3-5**

534 **Hz oscillations.**

535 (A) Example whole cell recording from a V1 layer 2/3 excitatory neuron during wakefulness,  
536 simultaneously recorded with the local electroencephalogram (ECoG, top) and the treadmill motion  
537 (locomotion, bottom). The second trace from the top represents the correlation between the ECoG

538 and the membrane potential (Vm) measured with the whole-cell recording. Grey highlights indicate  
539 times when 3-5 Hz oscillations were observed in the neuron's Vm.

540 (B) Simultaneous V1 ECoG (top) and whole-cell recordings (bottom) from V1 L2/3 excitatory (left), PV+  
541 (center), and SOM+ (right) neurons during Vm 3-5 Hz oscillations. During Vm 3-5 Hz oscillations, the  
542 ECoG also displays prominent 3-5 Hz oscillations.

543 (C) Plots of the mean change in Vm baseline during 3-5 Hz oscillations (left) and mean oscillation trough  
544 to peak amplitude (right) for excitatory (black, n=40), PV+ (red, n=6), and SOM+ (blue, n=7) neurons.  
545 Error bars represent SEM. PV neurons experienced greater changes in trough to peak amplitude  
546 (one-way ANOVA,  $p=0.01$ ) than excitatory neurons (Tukey-HSD,  $p=0.01$ ) and SOM+ neurons  
547 (Tukey-HSD,  $p=0.04$ ) during Vm 3-5 Hz oscillations. Change in Vm baseline was unchanged between  
548 neuronal types (one-way ANOVA,  $p=0.10$ ).

549 (D) Plots of mean frequency (left) and duration (right) of 3-5 Hz oscillatory periods in excitatory (black,  
550 n=40), PV+ (red, n=6), and SOM+ (blue, n=7). Error bars represent SEM. Oscillation frequency and  
551 duration was unchanged between neuronal types (one-way ANOVA,  $p=0.55$  &  $p=0.43$ ,  
552 respectively).

553

554 **Figure 2. Vm 3-5 Hz oscillations occur synchronously in V1 L2/3 neurons and decrease spontaneous**  
555 **excitatory neuronal output.**

556 (A) The mean ECoG (top) and Vm (bottom) during a single period of a Vm 3-5 Hz oscillation for  
557 excitatory (black, n=40), PV+ (red, n=6), and SOM+ (blue, n=7) neurons. For the ECoG traces, the  
558 colored line represents the mean ECoG z-score of all the neurons, and each light gray trace is the  
559 mean ECoG z-score trace from an individual neuron. For the Vm traces, the colored line represents  
560 the mean Vm from all cells, and the shaded region represents  $\pm$ SEM.

561 (B) The mean ECoG-Vm phase offset histogram between 3-5 Hz oscillations detected simultaneously in  
562 the ECoG and Vm traces for excitatory (black, n=40), PV+ (red, n=6), and SOM+ (blue, n=7) neurons.  
563 The dark line represents the mean phase offset in degrees between the ECoG and the Vm, and the  
564 shaded region represents  $\pm$ SEM.

565 (C) The mean spontaneous firing rate of excitatory (black, n=40), PV+ (red, n=6), SOM+ (n=7) during  
566 periods without (no osc.) and with (osc.) Vm 3-5 Hz oscillations. 3-5 Hz oscillations significantly  
567 reduced the spontaneous firing rate of excitatory (WSRT,  $p=0.002$ ) but not PV+ neurons (WSRT,  
568  $p=0.13$ ) and SOM+ neurons (WSRT,  $p=0.25$ ).

569

570 **Figure 3. Vm 3-5 Hz oscillations reduce excitatory neuron responsiveness to preferred stimuli during**  
571 **passive viewing of drifting gratings**

572 (A) Simultaneous recordings of the Vm from a layer 2/3 excitatory neuron, local ECoG, visual  
573 stimulations, and animal locomotion as an awake animal was shown drifting gratings. Full -field  
574 drifting grating presentations lasted 1.5 seconds and were interspersed with 1.5 seconds of an  
575 isoluminant gray screen. See Methods for more information about the visual stimuli. Visual stimulus  
576 presentation times are highlighted in gray, and dotted lines underline periods of 3-5 Hz oscillations  
577 in the Vm recording.

578 (B) Example of an excitatory neuron's Vm in response to its preferred visual stimulus in the absence  
579 (top) and during (bottom) Vm 3-5 Hz oscillations. The dotted lines underline periods of 3-5 Hz  
580 oscillations in the Vm recording.

581 (C) The mean orientation tuning of excitatory (top, n=40), PV+ (middle, n=6), SOM+ (bottom, n=7)  
582 neurons during (grey) and in the absence of (black) 3-5 Hz oscillations. The firing rate at the  
583 preferred angle was significantly larger in the absence of oscillations for excitatory neurons (WRST, p



584 =  $8.1 \times 10^{-5}$ ), but not for PV+ (WRST,  $p = 0.07$ ) and SOM+ (WRST,  $p = 0.63$ ) neurons. Shaded regions  
585 indicate  $\pm$ SEM.

586

587 **Figure 4. Prevalence and timing of 3-5 Hz oscillations during passive viewing**

588 (A) The number of oscillations per minute during passive viewing (darker) and spontaneous activity (Sp.,  
589 lighter) for excitatory (grey), PV+ (red), and SOM+ (blue) neurons. The incidence of oscillations was  
590 different for all neuron types during passive viewing and spontaneous activity (excitatory, WSRT,  $p =$   
591  $1.5 \times 10^{-5}$ ; PV+, WSRT,  $p = 0.025$ ; SOM+, WSRT,  $p = 0.038$ ).

592 (B) The mean probability of 3-5 Hz oscillations occurring during and after a visual stimulus for  
593 excitatory, PV+, and SOM+ neurons. Shaded regions indicate  $\pm$ SEM. Inset: the probability of an  
594 oscillation occurring for all neuron types when a visual stimulus was on and off. Oscillations  
595 occurred more frequently after visual stimulus offset than during visual stimuli presentations (WSRT,  
596  $p = 7.2 \times 10^{-9}$ ).

597 (C) The mean probability of 3-5 Hz oscillations occurrences was calculated during blocks of visual stimuli  
598 presentations grouped by the time of presentation (1<sup>st</sup> quartile = first quarter of visual stimuli  
599 shown) for all neurons ( $n = 31$ ). Recordings with fewer than 100 visual stimulus presentations were  
600 excluded (mean number of visual stimuli per neuron =  $176 \pm 20$ ). The probability of 3-5 Hz  
601 oscillations decreased over the course of visual stimulus presentations (one-way ANOVA,  $p = 7.7 \times 10^{-7}$ ;  
602 quartile 1 vs. quartile 4, WSRT Bonferroni Corrected,  $p = 0.00001$ ). Error bars represent  $\pm$ SEM.

603 (D) The probability of oscillation onset triggered at visual stimulus (green) and locomotion (tan) onset  
604 (colored) and offset (grey). The probability of oscillation initiation at visual stimulus onset was  
605 greater than that at visual stimulus onset, locomotion onset, and locomotion offset (WSRT  
606 Bonferroni Corrected,  $p = 0.024$ ,  $p = 0.0003$ ,  $p = 0.003$ , respectively). Error bars represent  $\pm$ SEM.

607

608 **Figure 5. 3-5 Hz oscillations occur predominately during visual stimulation while animals perform a**

609 **visual discrimination task**

610 (A) Example sub-threshold activity from a single neuron as animals performed the task. Visual stimuli  
611 timing, licking, and locomotion were recorded simultaneously. Arrows indicate instances of 3-5 Hz  
612 oscillations in the whole-cell recording.

613 (B) The mean probability of 3-5 Hz oscillations occurring during a trial of the go/no-go task (n=21  
614 neurons). Periods where visual stimuli were on and off are marked at the top. The response time,  
615 when the animal must report its decision, is denoted in the blue region. Shaded regions indicate  
616  $\pm$ SEM. Inset: the probability of an oscillation occurring when a visual stimulus was on and off. In  
617 contrast to passive viewing, 3-5 Hz oscillations occurred more frequently during visual stimuli  
618 presentations than during inter-trial intervals (WSRT,  $p = 0.026$ ).

619 (C) Comparison of the mean 3-5 Hz oscillation frequency (left, WRST,  $p = 0.8$ ) and duration (right, WRST,  
620  $p = 0.009$ ) in neurons recorded from animals during active behavior (red, n=21) and passive viewing  
621 (blue, n=53).

622 (D) Comparison of the mean probability of 3-5 Hz oscillations occurring in neurons recorded from  
623 animals during active behavior (red, n=21) and passive viewing (blue, n=53) while a visual stimulus is  
624 on (left, WRST,  $p = 0.001$ ) and off (right, WRST,  $p = 0.007$ ).

625 (E) The mean firing rate evoked by optimal visual stimuli (left, WSRT,  $p = 0.001$ ) and orthogonal visual  
626 stimuli (right, WSRT,  $p = 0.68$ ) when 3-5 Hz oscillations were present (osc.) or absent (no osc.) in  
627 neurons recorded from animals during active behavior (n=21). Error bars represent  $\pm$ SEM.

628 (F) The mean probability of 3-5 Hz oscillations occurrences was calculated during blocks of visual stimuli  
629 presentations grouped by the quartile of visual stimulus presentations. Neurons with less than 100  
630 stimuli were excluded (n=15, mean number of visual stimuli per neuron =  $127 \pm 14$ ). No change in



631 probability of 3-5 Hz oscillations was observed over the course of visual stimulus presentations  
632 (repeated measures one-way ANOVA,  $p = 0.099$ ). Error bars represent  $\pm$ SEM.

633

634 **Figure 6. Behavioral response modulates oscillation probability and timing**

635 (A) The mean probability of 3-5 Hz oscillations occurring during go trials (hits, black; false alarms (FA))  
636 and no-go trials (correct rejections (CR), dark lines; misses, light lines) ( $n=21$  neurons). Compared to  
637 CR trials, oscillations were less likely to occur during hit trials (WSRT Bonferroni corrected,  $p = 0.046$ )  
638 and FA trials (WSRT Bonferroni Corrected,  $p = 0.04$ ). Error bars represent  $\pm$ SEM.

639 (B) The mean duration of 3-5 Hz oscillations during go trials (hits, black; false alarms (FA)) and no-go  
640 trials (correct rejections (CR), dark lines; misses, light;  $n=21$  neurons). Oscillations were shorter  
641 during hit trials than during CR trials (WRST Bonferroni Corrected,  $p = 0.035$ ). Error bars represent  
642  $\pm$ SEM.

643 (C) Comparison of oscillation (dark grey) and licking (blue) timing during hit, FA, CR and miss trials ( $n=21$   
644 neurons). Oscillations tend to begin after licking onset in hit (WSRT,  $p = 0.01$ ) and FA (WSRT,  $p =$   
645  $0.001$ ) trials. In CR trials with premature licking, oscillations tend to begin after licking offset (WSRT,  
646  $p = 0.031$ ). Visual stimulus on time is indicated at the top. The response time is indicated in the light  
647 blue box. Error bars represent  $\pm$ SEM.

648

649 **Figure 7. 3-5 Hz oscillations are absent in V1 when animals perform an analogous auditory**  
650 **discrimination task**

651 (A) Example sub-threshold activity from a single neuron as animals performed the task. Auditory stimuli  
652 timing, licking, and locomotion were recorded simultaneously. Arrow indicates an instance of 3-5 Hz  
653 oscillations in the whole-cell recording.

654 (B) The mean probability of 3-5 Hz oscillations occurring during a trial of the auditory (n=7 neurons) and  
655 visual (n=21 neurons) go/no-go tasks. Periods where stimuli were on and off are marked at the top.  
656 The response time, when the animal must report its decision, is denoted in the light blue region.  
657 Shaded regions indicate  $\pm$ SEM.

658 (C) Comparison between the mean probability of 3-5 Hz oscillations during a trial (WRST,  $p = 0.003$ ),  
659 oscillation duration (WRST,  $p = 0.27$ ), oscillation onset latency from stimulus onset (WRST,  $p = 0.64$ ),  
660 and discriminability (WRST,  $p = 0.037$ ) during the auditory (red) and visual (blue) discrimination task.  
661 Error bars represent  $\pm$ SEM.

662

663 **Figure 3—figure supplement 1. Oscillations do not affect the orientation selectivity index of excitatory**  
664 **neurons**

665 (A) The orientation selectivity index of excitatory neurons was calculated for excitatory neurons during  
666 passive viewing when 3-5 Hz Vm oscillations were present (osc.) or not present (no osc.; see  
667 methods for calculation). Orientation selectivity was not changed by the presence of 3-5 Hz Vm  
668 oscillations (n = 40; WSRT,  $p = 0.93$ ).

669

670 **Figure 5—figure supplement 1. Task schematic and animal learning curves**

671 (A) Left: Schematic of the training set-up. Right: Task schematic. Visual stimuli were presented for three  
672 seconds. In go trials, 45° gratings were displayed and a water reward was issued two seconds after  
673 stimulus onset. During no-go trials, 135° gratings were displayed and no reward was issued. Animal  
674 response (licking) was recorded during the response period to assess correct behavior. For more  
675 details, see Materials and Methods.

676 (B) The mean discriminability of animals during training, which is a measure of animal performance (n =  
677 17 mice). Black line: the mean performance of all animals on a given session date. Light grey lines:

678 the mean performance of a single animal on a given session date. Animals were recorded once their  
679 mean discriminability surpassed  $D' = 1.7$  (Monte Carlo Simulation,  $p = 0.01$  random behavior).

680 (C) The mean lick rate of animals during go (left) and no-go (right) trials during their first training session  
681 (darker) and last session (lighter).

682

683 **Figure 5—figure supplement 2. Locomotion does not change 3-5 Hz oscillation probability during**  
684 **active behavior.**

685 (A) The mean probability of 3-5 Hz oscillations occurring during trials of the visual discrimination task  
686 with locomotion (red) and without locomotion (blue) ( $n = 21$  neurons). Visual stimuli on and off times  
687 are shown at the top. The response time is indicated by the blue box. Shaded regions represent  
688  $\pm$ SEM.

689 (B) The mean oscillation probability (left) and oscillation onset latency from visual stimulus onset (right)  
690 during trials with (red) and without (blue) locomotion ( $n = 21$  neurons). No changes in oscillation  
691 probability (WSRT,  $p = 0.76$ ) and oscillation onset latency (WSRT,  $p = 0.56$ ) were observed between  
692 trials with locomotion and without locomotion.

693

694 **Figure 4—figure supplement 1. Oscillation timing is shifted proportionally when the visual stimulus**  
695 **duration is increased.**

696 (A) The mean probability of 3-5 Hz oscillation onset during and after drifting gratings presents for three  
697 seconds ( $n = 9$  neurons). Shaded regions indicate  $\pm$ SEM.

698 (B) The mean probability of 3-5 Hz oscillations during and after drifting gratings presented for three  
699 seconds ( $n = 9$  neurons). Shaded regions indicate  $\pm$ SEM. Inset: the probability of an oscillation  
700 occurring when a visual stimulus was on and off. Oscillations occurred more frequently between  
701 visual stimuli presentations than during visual stimuli presentations (WSRT,  $p = 0.004$ ).

702

703 **Figure 4—figure supplement 2. Probability of oscillation onset at visual stimulus and locomotion onset**  
704 **and offset.**

705 (A) The mean probability of 3-5 Hz oscillation onset at visual stimulus onset (top) and offset (bottom)  
706 for excitatory (black, n=40), PV+ (red, n=6), and SOM+ (blue, n=7) neurons. Shaded regions indicate  
707  $\pm$ SEM.

708 (B) The mean probability of 3-5 Hz oscillation onset at locomotion onset (top) and offset (bottom) for  
709 excitatory, PV+, and SOM+ neurons. Shaded regions indicate  $\pm$ SEM.

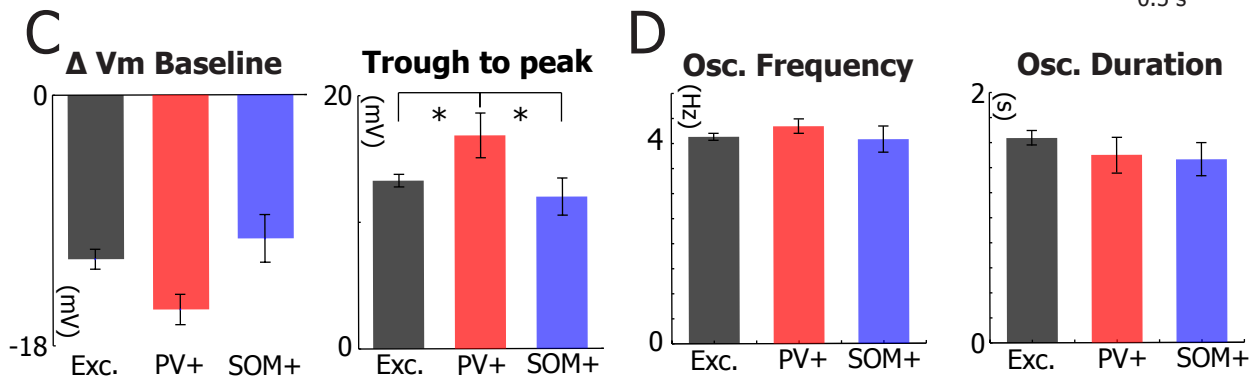
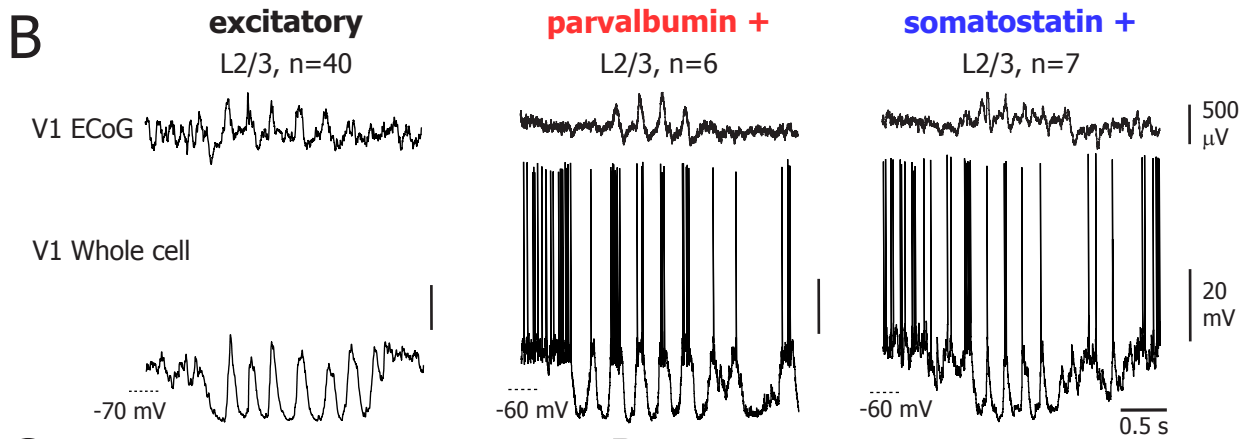
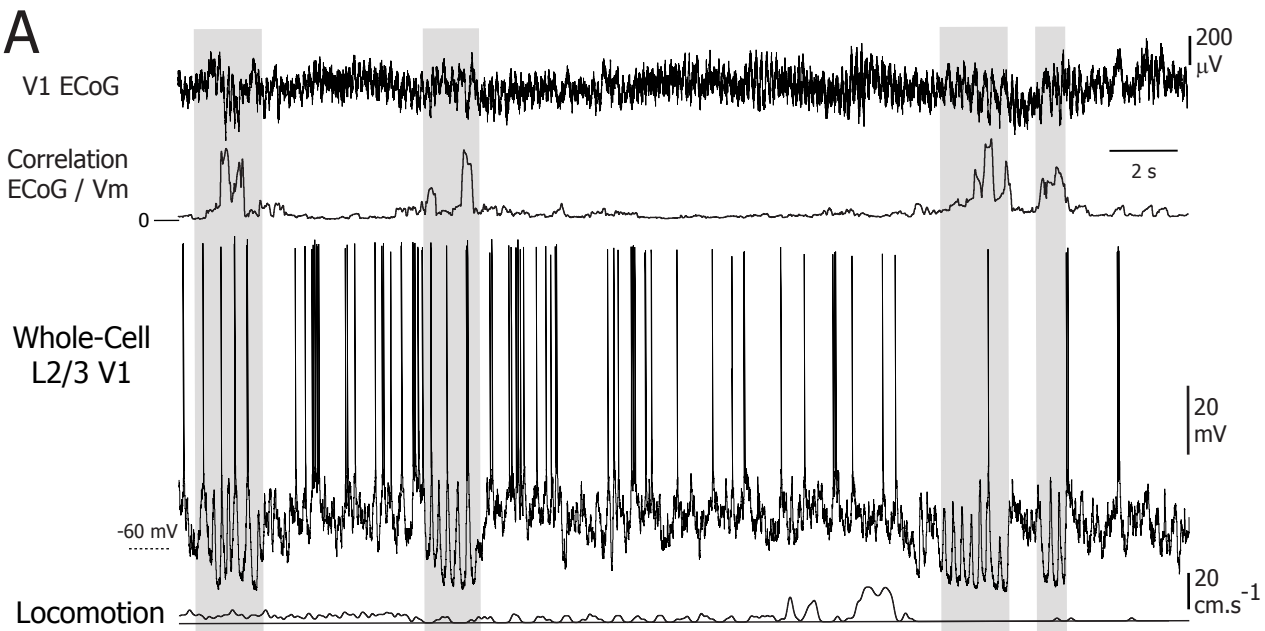


Figure 2.

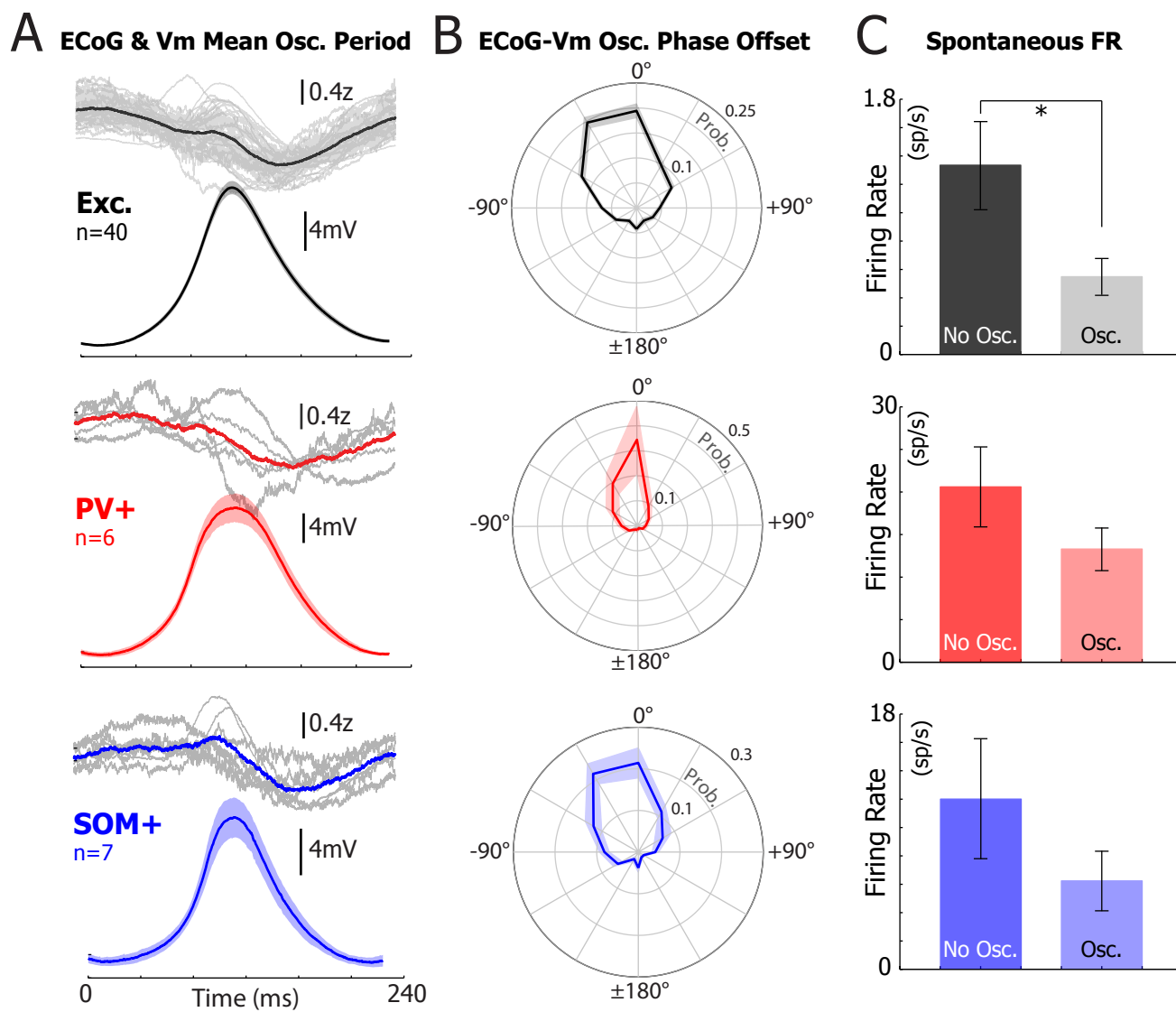


Figure 3.

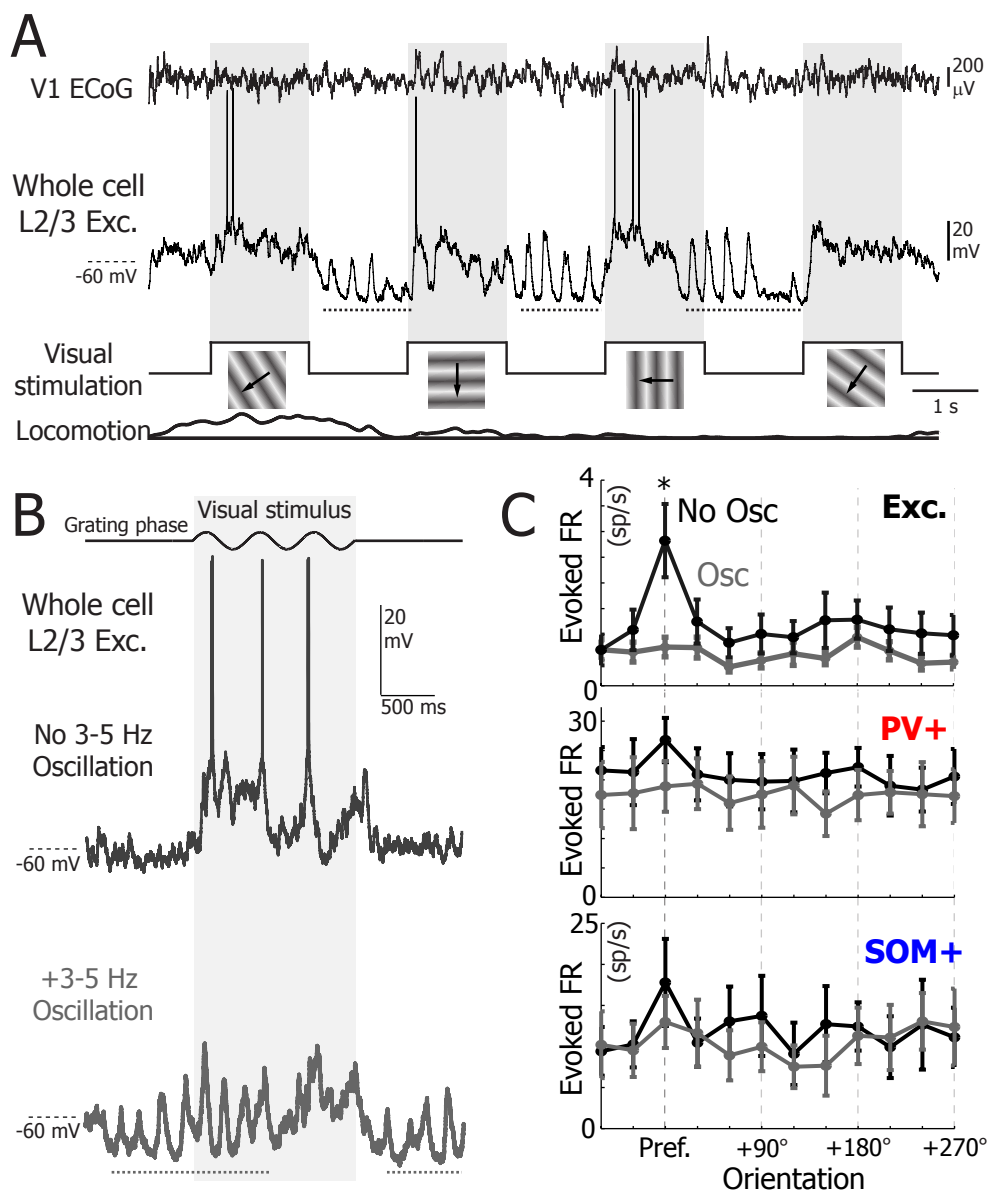


Figure 4

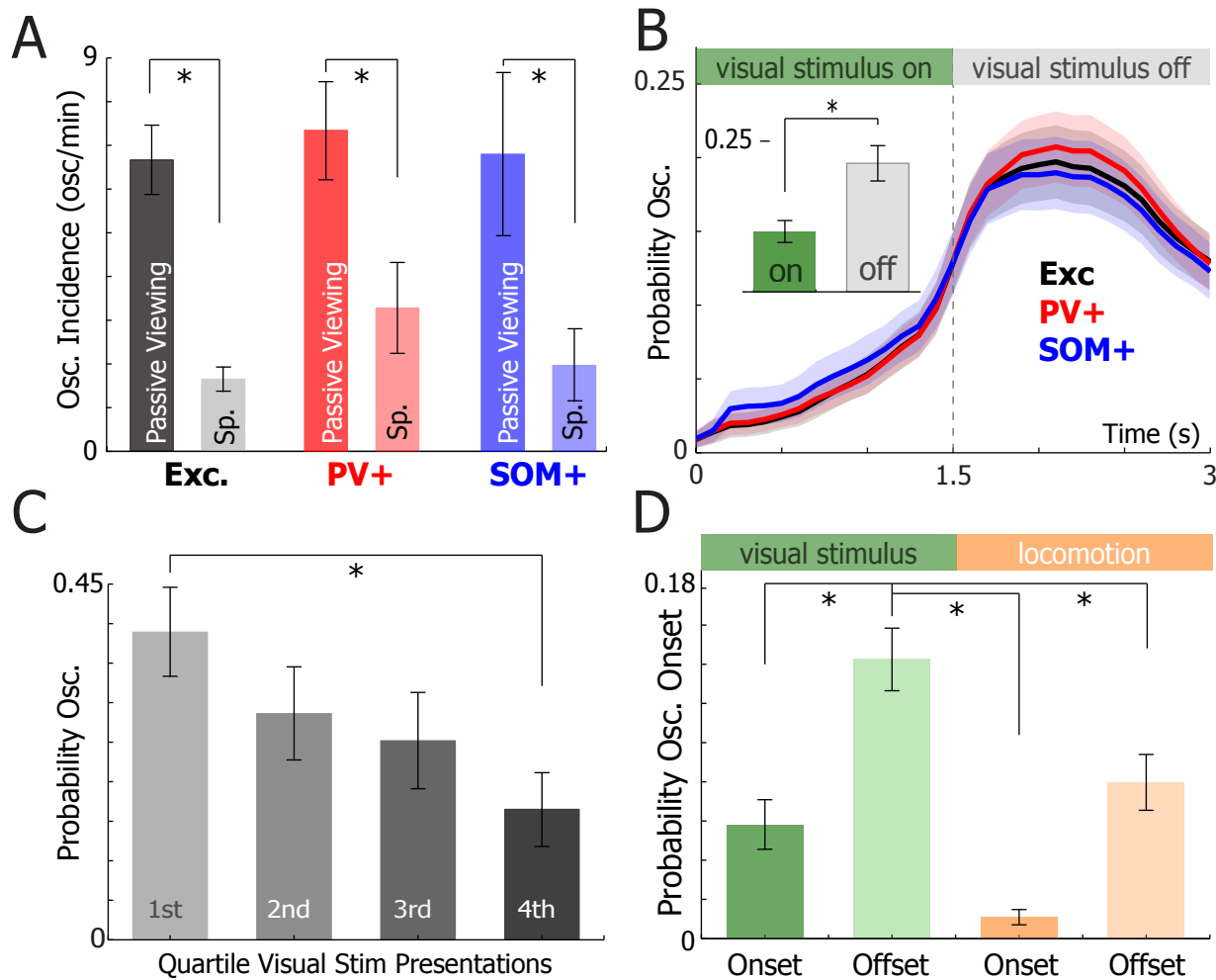




Figure 5.

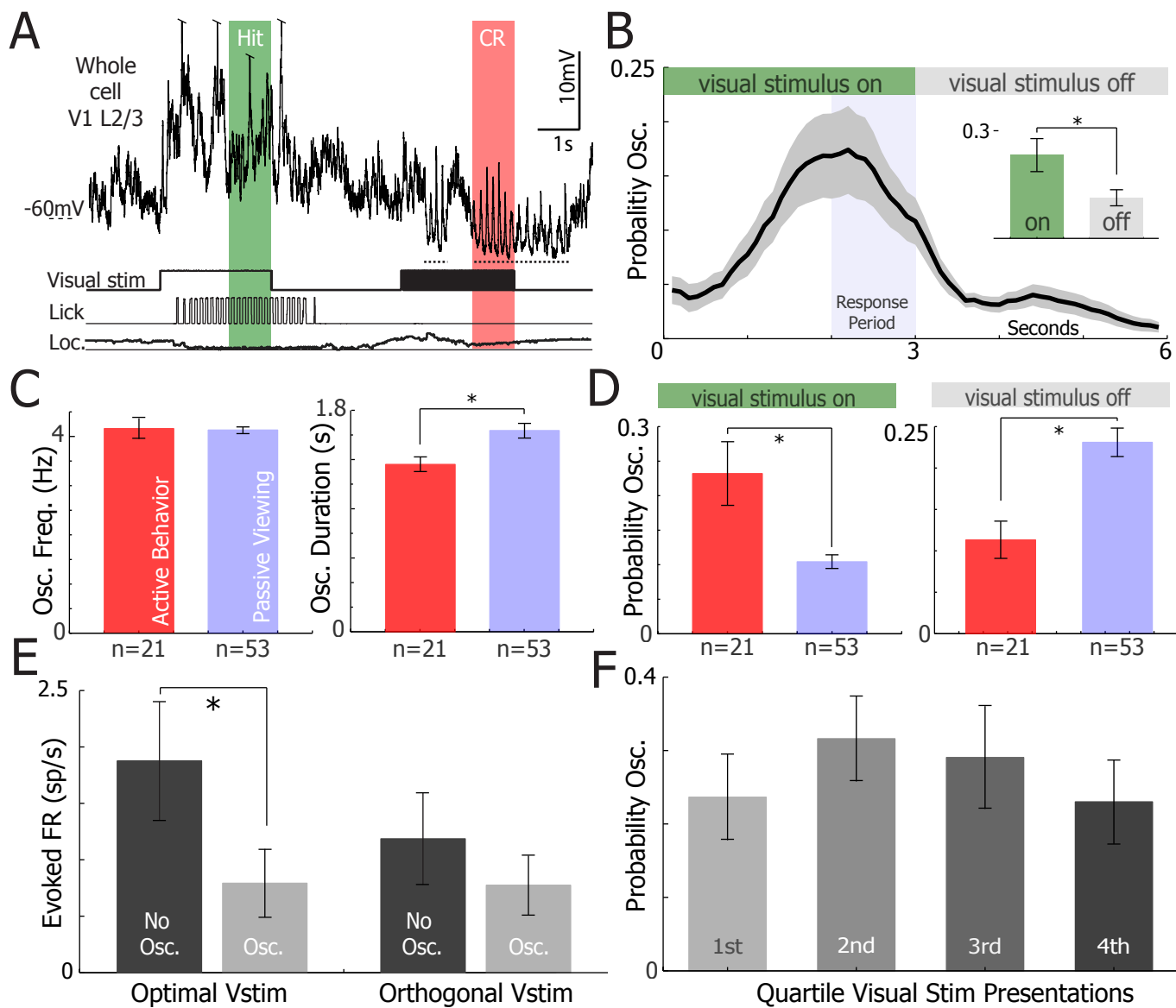


Figure 6

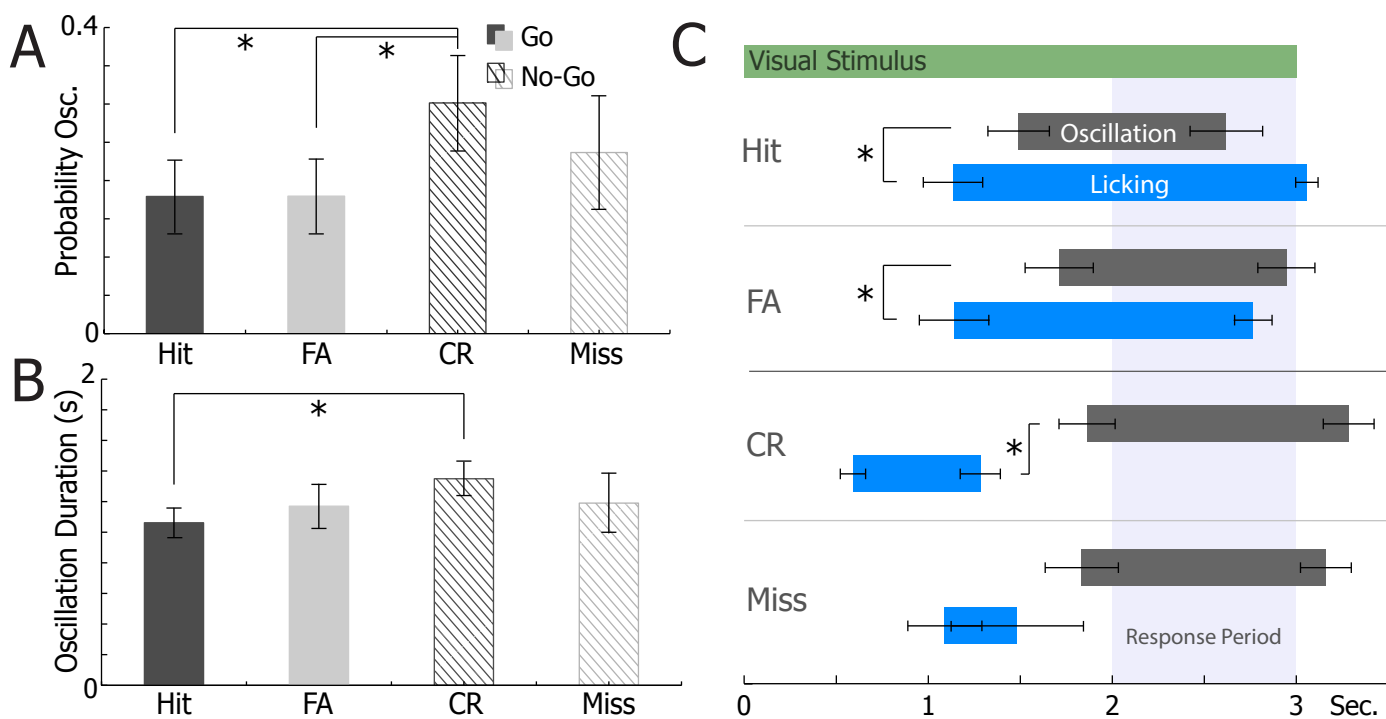


Figure 7

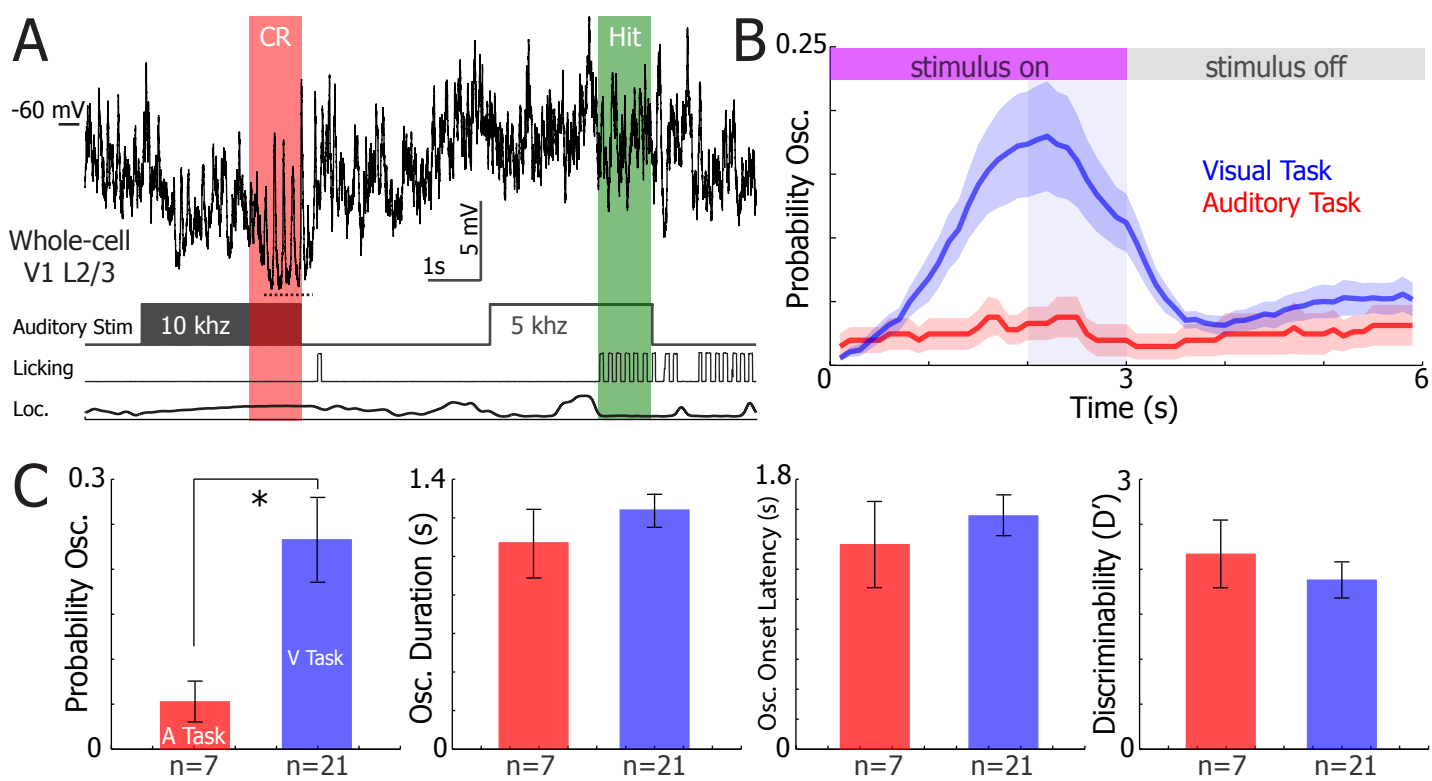


Figure 3-- figure supplement 1

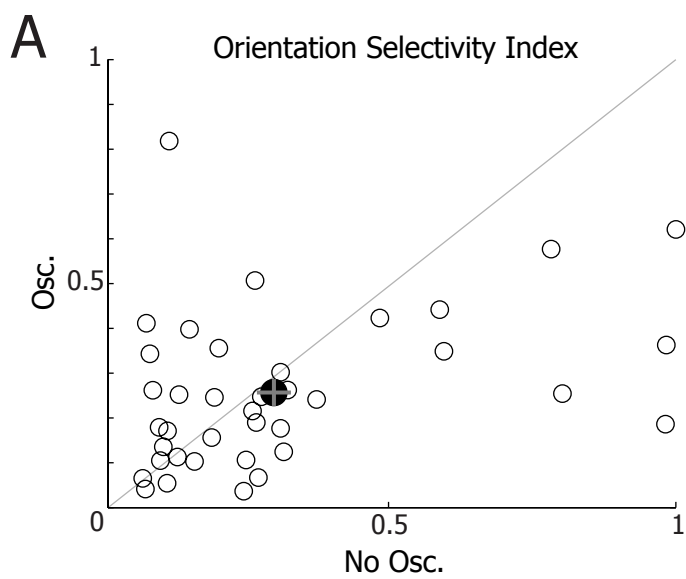


Figure 4-- figure supplement 1

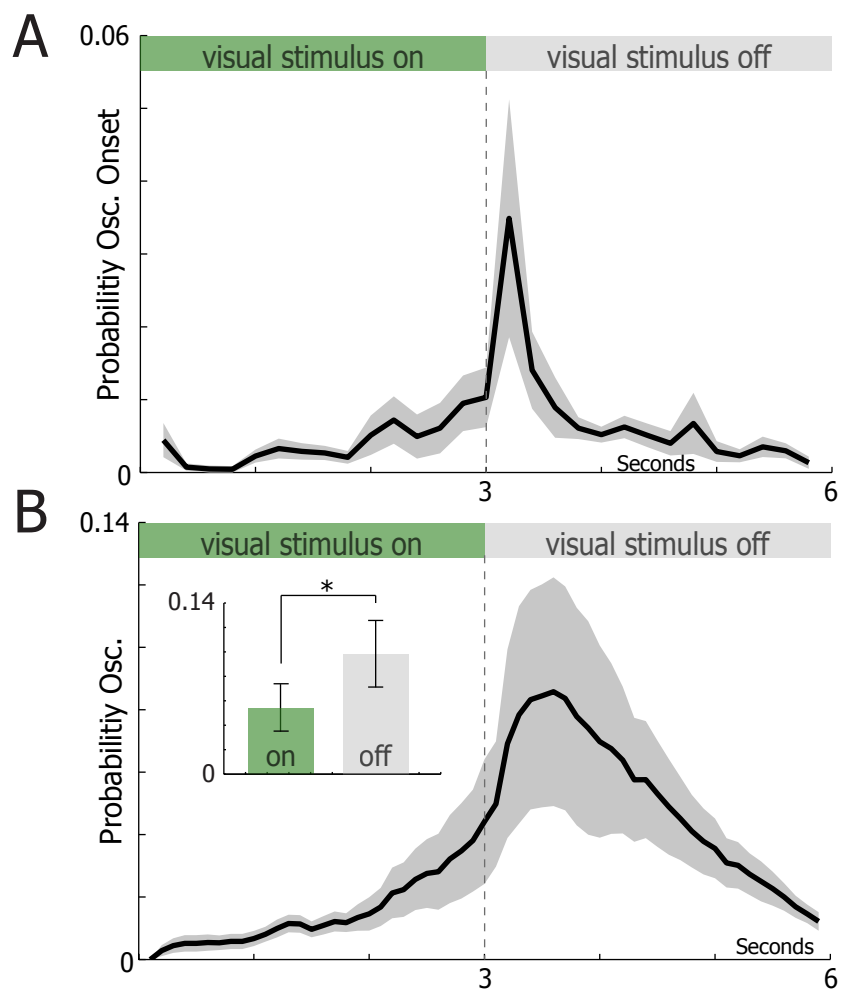


Figure 4-- figure supplement 2

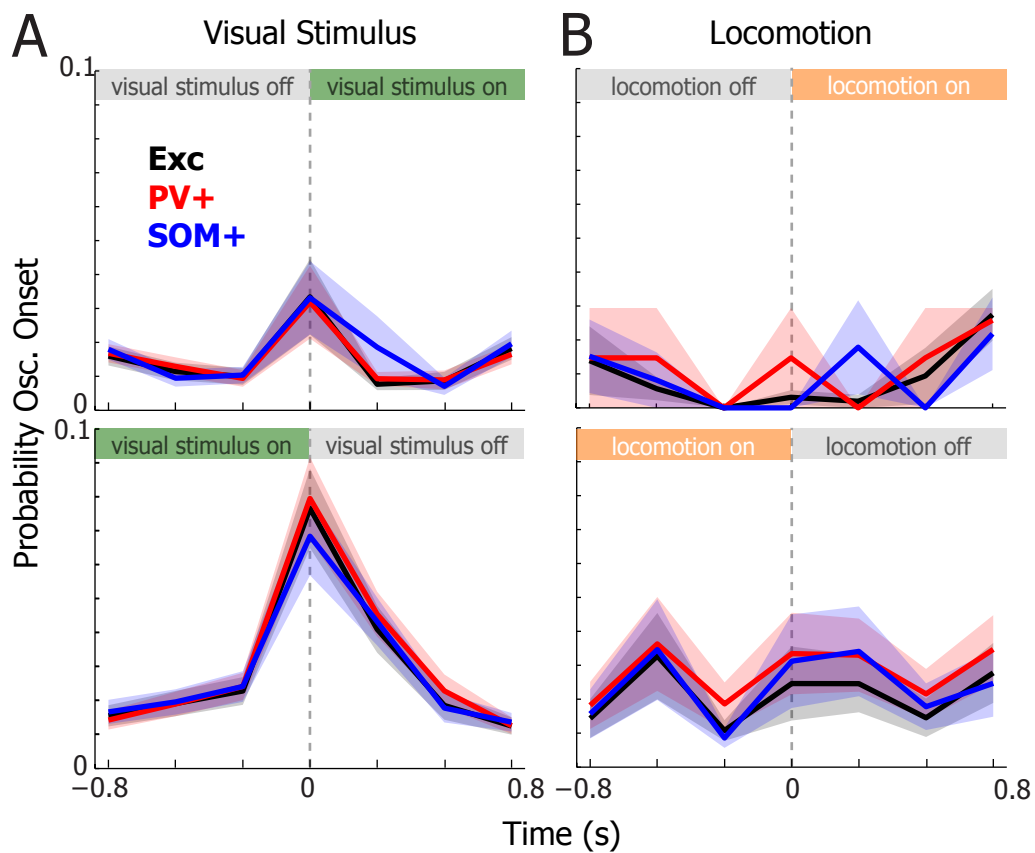


Figure 5--supplementary figure 1

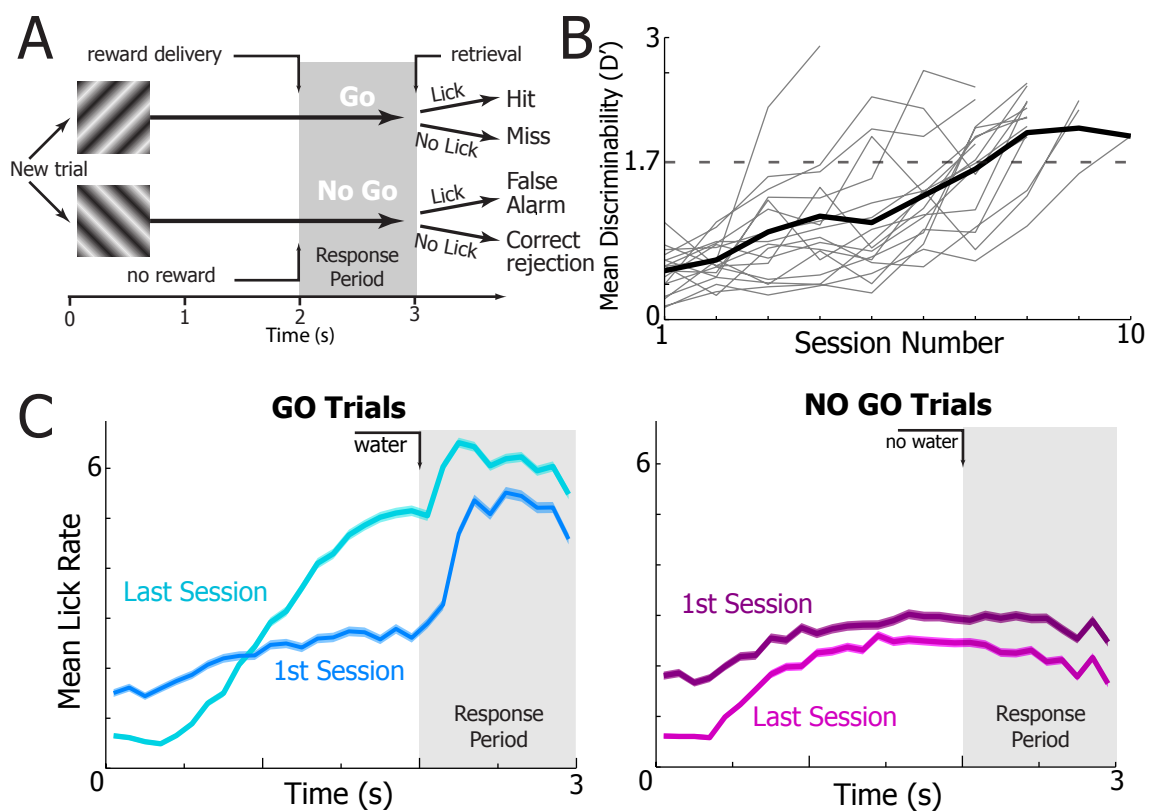


Figure 5--supplementary figure 2

